Clays and Clay Minerals, Vol. 48, No. 5, 528–536, 2000.

EVALUATION OF THE ACIDITY OF PILLARED MONTMORILLONITES BY PYRIDINE ADSORPTION

M.R. Sun Kou, S. Mendioroz, and V. Muñoz[1]

Instituto de Catálisis y Petroleoquímica, Campus UAM, Cantoblanco 28049 Madrid, Spain
[1] Departamento de Química Inorgánica y Química Técnica U.N.E.D., Senda del Rey s/n 28040 Madrid, Spain

Abstract—Two series of pillared clays were prepared from a purified montmorillonite (95%) from La Serrata of Nijar, Spain, and polycations of Al and Zr using various methods. The effect of both the pillaring cation and the procedure of preparation on the physicochemical characteristics of the resulting materials was studied. Changes in texture were determined by X-ray diffraction (XRD) and N_2 adsorption at 76 K and changes in acidity were determined by thermogravimetry following pyridine adsorption at room temperature and further desorption at a constant heating rate of 10 K min^{-1} in the range of 298–623 K. The relation between the size and charge (n/q) of the pillaring cation, which is dependent on the degree of cation hydrolysis, is the main factor affecting pore size and acidity of the synthesized materials. The pH of the pillaring solution affects the stability of the parent clay and the properties of the pillared clay. Below a pH of 3 and depending on contact time, the montmorillonite may delaminate and partially dissolve to produce products that affect the properties of the resulting materials. Microporosity increases for both Al or Zr-pillared clays. For Zr-pillared clays, microporosity is accompanied by changes in the mesoporosity and macroporosity as a result of clay delamination. Acidity dramatically increases by pillaring, especially strong acidity, and the acid strength distribution depends on starting salt concentration, aging time, and temperature.

Key Words—Acidity, Al-Pillared Montmorillonite, Mesoporous Materials, Pyridine Adsorption, Zr-Pillared Montmorillonite.

INTRODUCTION

Pillared smectites are a highly porous cross-linked clay product, generally prepared by cation exchange of the smectite with polynuclear cations, which are incorporated and immobilized in the interlamellar space, leaving part of the interlayer region open for adsorption and catalysis. The use of pillared clays as acid catalysts could benefit from knowledge of the number, strength, and nature of the acid sites involved. However, the characterization of these acidity characteristics is not easy.

Clays, in general, have both Brönsted and Lewis-type acidity. Brönsted acidity essentially results from the dissociation of absorbed H_2O molecules. This dissociation is induced by the electric field of the exchangeable cations to which they are associated. The presence of surface sylanol groups (≡Si-OH), resulting from broken ≡Si-O-Si≡ bonds in the tetrahedral sheet, either via treatment with acids or by extended contact with water by the clay (Barrer, 1984) also contributes to Brönsted acidity. In contrast, Lewis acidity results not only from low-coordinated Al and/or Mg on the crystal edges, but also, and most importantly, from the isomorphous substitution of Si^{4+} by Al^{3+} and of Al^{3+} by Mg^{2+}. These substitutions create Lewis-base sites in clays, particularly in smectites, and Lewis-acid sites in the interlayer.

Previously, acidity in pillared materials was thought to be of the Lewis-acid type and resulting mainly from dehydroxylation of the hydrated large interlayer cations. However, when heated, these polyoxycations form oxide clusters (although they contain Lewis-acid sites) and protons, which are retained as charge-compensating cations (Occelli, 1986) and which possibly enhance the Brönsted acidity. On the other hand, these protons can migrate to octahedral holes, thereby becoming inaccessible and finally resulting in the degradation of the octahedral sheet (Vaugham *et al.,* 1981; Occelli and Tindwa, 1983). Recent reports (Bodoardo *et al.,* 1994) suggest that the host-guest interactions between clays and intercalated compounds enhance reactivity and modify the physicochemical properties of the intercalation compounds. Thus, intercalation significantly increases the acid properties of the incorporated cations (Hashimoto *et al.,* 1996), inducing hydroxyl groups to be easily dissociated, and creating Brönsted acidity. The number of Brönsted-acid sites decreases with an increase in temperature and these sites are practically lost between 573–773 K (Vaugham *et al.,* 1981).

Carrado *et al.* (1990) stated that Lewis acidity in pillared clays is associated with the interlayer cations, and this was supported by Tichit *et al.* (1991). Ming-Yuan *et al.* (1988) concluded that acidity varies with the type of hydroxycation (Ti > Zr > Al > Fe), and acidity increases with the number of pillars and decreases with calcination temperature.

By comparing clays intercalated with aluminum, zirconium, and chromium-hydroxy oligomers, Auer and Hofmann (1993) recently concluded that the metal

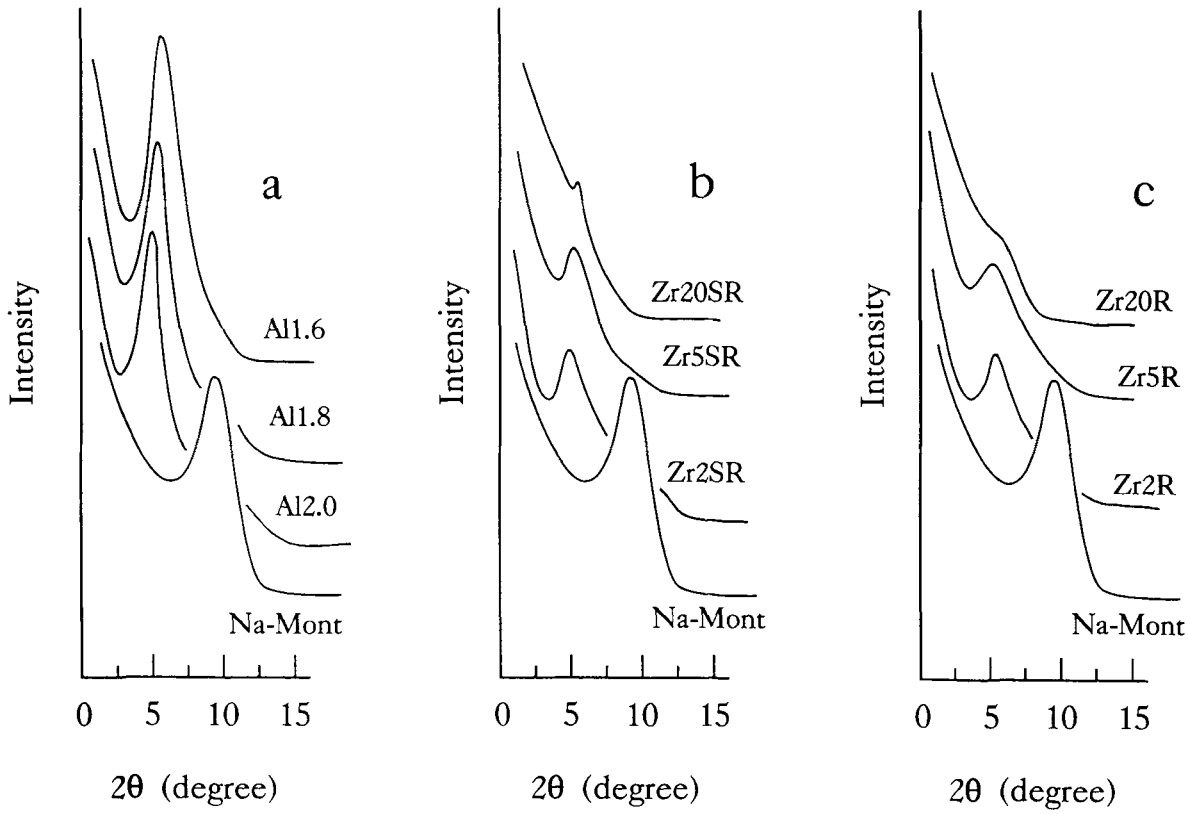

Figure 1. X-ray difractograms of pillared montmorillonites: a) Al-series; b) ZrSR-series; c) ZrR-series.

concentration in the dispersion of the oligomer solution and clay-mineral suspension influences the pillar density by increasing the degree of ion exchange. Because the Lewis-acid sites are mainly located in the pillars, a parallel increase in the number of Lewis-acid sites with the metal concentration is expected. In contrast, the number of Brönsted-acid sites is nearly constant, because they exist mainly in the 2:1 layers. Bodoardo *et al.* (1998) more recently reported that pillars and clay layers show synergetic effects, involving both acidity and reactivity of the pillared clay: seven hydroxyl sites were identified, some of these hydroxyl groups undergo proton transfer with strong bases like ammonia.

Acid-site accessibility (resulting from stacking disorder) may also affect the total number of measured acid sites, with a greater number of sites in pillared bentonite than in delaminated catalysts with the same surface area. Therefore, it is difficult to predict a preparative method or included cation for generating new acid centers. Thus, a reliable method would be useful to evaluate the presence of acid centers following synthesis. One such method which shows promise involves pyridine chemisorption. The purpose of this study is to determine the effect of various synthesis parameters on the acidity produced by the intercalation of Al and Zr hydroxycations. We explore the use of pyridine adsorption as a method to evaluate changes in the samples during synthesis.

EXPERIMENTAL

Materials

The starting mineral was a montmorillonite-rich bentonite from La Serrata of Nijar, (Southeastern Spain) supplied by Minas of Gador S.A. The montmorillonitic fraction (<2 μm), separated by conventional sedimentation following dispersion in deionized water, had a cation-exchange capacity (CEC) of 61.6 meq per 100 g of clay. The surface area was 87 m^2 g^{-1} and the pore volume was 0.121 cm^3 g^{-1}. The structural formula, calculated by the Ross and Hendricks method (1945) is: $^{IV}(Si^{4+}_{7.74}Al^{3+}_{0.26})^{VI}(Al^{3+}_{2.5}Fe^{3+}_{0.25}Mg^{2+}_{1.30}Ni^{2+}_{0.003})O_{20}(OH)_4(Ca^{2+}_{0.21}Na^{+}_{0.85}K^{+}_{0.11})_{EC}$ where EC is for the exchangeable cations. To prepare the pillared materials, the mineral was exchanged with a 1 M solution of NaCl to obtain Na-rich montmorillonite (Na-Mont). The homoionic material had a surface area (S) determined by the BET method (Brunauer *et al.*, 1938), (S_{BET}), of 77 m^2 g^{-1}, pore volume (Vp) of 0.093 cm^3 g^{-1}, and an X-ray *d* value for the (001) of 12.01 Å (Figure 1).

https://doi.org/10.1346/CCMN.2000.0480505 Published online by Cambridge University Press

As an Al-pillaring agent, a 0.2 M $AlCl_3 \cdot 6H_2O$ solution treated with a 0.5 M NaOH solution as a neutralizing agent was used following the method described by Lahav *et al.* (1978), Yamanaka and Brindley (1978), Tokarz and Shabtai (1985), Sterte (1986), and Pesquera *et al.* (1991). The molar concentration ratio between hydroxide and aluminum ions used was either 1.6, 1.8, or 2.0, and these values are hereafter used to differentiate the samples. The amount of 20 meq Al/g of clay was always used in the preparation.

$ZrOCl_2 \cdot 8H_2O$ (Aldrich Chemicals) was used to prepare the Zr-pillaring polycations. Zr-pillared montmorillonites were prepared by the following two methods: 1) adapted from Yamanaka and Brindley (1979) with slight modification by adding appropriate volumes of $ZrOCl_2 \cdot 8H_2O$ (0.1 M) to 5 g of Na-Mont and continuous stirring for 24 h at room temperature, and 2) adopted from Bartley and Burch (1985), 5 g of Na-Mont were added to appropriate volumes of $ZrOCl_2 \cdot 8H_2O$ (0.1 M), which were previously refluxed for 24 h. The suspension was then stirred for another 24 h at room temperature. After preparation by either method, the clay suspensions were dialyzed against distilled water (1 L/g of clay) until free of chlorides. Finally, the samples were freeze-dried and calcined at 623 K for 2 h to fix the oligomer to the clay.

We follow the following labeling scheme: the pillared clay is identified based on pillar chemistry (*e.g.,* Zr), followed by the concentration of the dispersion (*e.g.,* 2, 5, or 20 meq per g of clay), and followed by the oligomer preparative method (*e.g.,* R = reflux, SR = without reflux). Thus, Zr2R indicates a Zr pillar prepared from a 2 meq per g clay solution by a reflux method. All materials were tested in powder form.

Analysis and pyridine adsorption

Al and Zr were analyzed by inductively coupled plasma (ICP) emission spectrometry in a Perkin Elmer Plasma 40 instrument, using Ar as the plasmogene. X-ray diffraction (XRD) analysis used a Siemens Diffractometer model Kristalloflex D-500 and CuKα radiation. The spectra were acquired at 2° per min from 2θ = 2–75°. Surface area and porosity were determined by nitrogen adsorption at 76 K, using a Micromeritics ASAP 2000 sorptometer. Prior to N_2 exposure, the samples were outgassed at 473 K for 16 h. In surface-area calculations, 0.162 nm^2 was used for the cross-sectional area of the adsorbed N_2 molecule. To evaluate microporosity, the t-method, (Lippens and de Boer, 1965) and the standard curve from Harkins and Jura (1944) were used. This standard t-curve was also used to study pore-size distribution by the BJH method (Barret *et al.,* 1951).

Pyridine (C_5H_5N) adsorption was performed with a Perkin-Elmer TGS-2 thermobalance with a Data Station 3600 and temperature controller System 7/4. The system sensitivity is not <0.2 μg. The sample was initially degassed for 3 h in a 50 cm^3/min N_2 stream at 623 K, then cooled and exposed for 3 h to a pyridine-saturated N_2 stream at room temperature to obtain the corresponding adsorption isotherm. Then, the pyridine flow was stopped, and the N_2 stream continued to remove the physisorbed fraction to equilibrium. From the fraction of pyridine retained, the total number of acid centers per gram of sample was calculated. Then, the sample was heated at a constant rate of 10 K min^{-1} to 623 K. The remaining pyridine at various temperatures was taken as a measure of the acid-strength distribution of the sample.

RESULTS

In Figure 1 the diffractograms corresponding to the resulting materials, together with the pattern of Na-Mont as a comparison, are included. A shift towards larger basal spacing in all samples after pillaring is observed.

S_{BET} and porosity

Figure 2 shows the N_2 adsorption-desorption isotherms for all studied materials, and the resulting textural characteristics are given in Table 1. To evaluate microporosity (Table 1), t-plots were derived from the isotherms by using the statistical curve from Harkins and Jura (1944) as a standard. Table 1 shows no significant change in the original texture of the Al-pillared clays from the pillaring process, except for an increase in microporosity; the external area remains nearly unchanged. Note that Zr2SR shows an external surface area similar to Na-Mont, but the remaining samples of the series show an increase, with the more drastic the treatment the greater the increase, thus indicating that the pillaring process affects the clay.

The resulting pore-size distributions as determined by the BJH method at the obtained isotherms are shown in Figure 3. Microporosity below 10 Å was assumed on the basis that adsorption is the only prevailing mechanism. Thus, the statistical t values (Harkins and Jura, 1944) are therefore relating to pore size. From 10 to near 20 Å, a cooperative mechanism of reversible condensation was assumed in addition to adsorption (Gregg and Sing, 1982). The pore-size distribution was determined by the BJH method and by taking into account the limitations of the Kelvin equation (Defay *et al.,* 1966) below 0.42 N_2 relative pressure, as is the case. The bimodal distribution obtained is typical for these materials.

Pyridine adsorption

Isotherms of pyridine as wt. % adsorbed *vs.* time are shown in Figure 4a for the Al series, and in Figure 4b and 4c for the SR and R series, respectively. For comparison, the isotherm corresponding to Na-Mont is also included. All samples, except Na-Mont, show

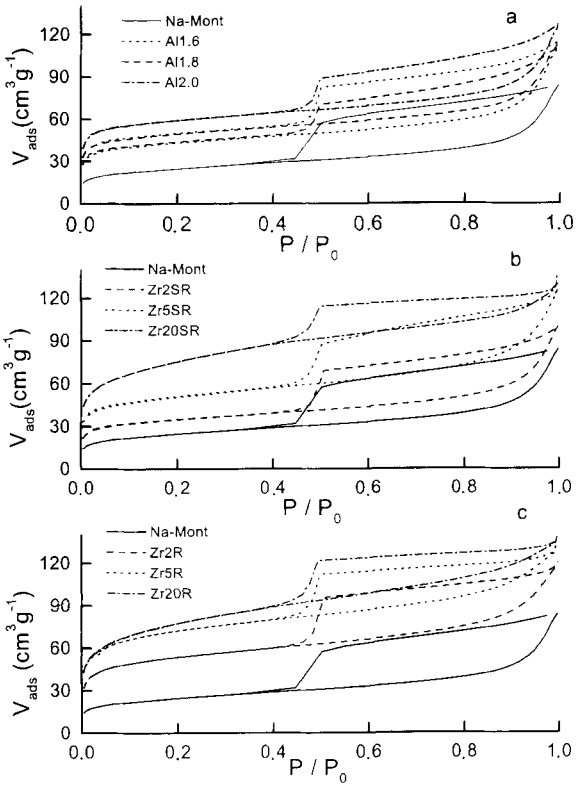

Figure 2. N_2 adsorption-desorption isotherms; adsorbed volume [V_{ads} in cm^3 g^{-1}] *vs.* relative pressure (P/P_0): a) Al-series; b) ZrSR-series; c) ZrR-series, under conditions of standard temperature and pressure (STP).

an S-shaped adsorption curve with three steps and with the extension of each region of the curve differing from sample to sample. The S-shaped curve involves an initial region of little adsorption, followed by a rapid increase in sorption with time, and a final nearly horizontal plateau corresponding to the saturation of the sample. No large differences are observed among the samples of series Al and ZrSR. However, the quantities of pyridine adsorbed by the R series were smaller, perhaps because the kinetics of adsorption were slower and saturation was not obtained under these experimentation conditions. Na-Mont shows at first, a slower adsorption than the remaining curves (extended through nearly 60 min), and afterwards, it increases nearly proportionally to exposure time, without reaching saturation during the experiment. This effect was observed by Barrer (1989, and references therein) for the non-specific adsorption of polar molecules by clays.

Total uptake (Table 2) is ascribed to both physisorption and chemisorption, whereas the values after room temperature desorption (column 4 in Table 2) are related only to chemisorption and are given as acid-site density. Pyridine uptake (Figure 4) increases with pillaring. The chemisorbed fraction increases with pillaring, but diminishes with the basicity and increases with the acidity of the pillaring solution to a limit (here at pH > 2.30). Once desorption equilibrium was reached, the samples were analyzed by thermal desorption at a constant rate by N_2 stream (see above). Table 3 shows acid-site densities at selected tempera-

Table 1. Physico-chemical characteristics of the materials.

[1]Sample	[2]pH	Metal (pillar) wt. %	*d*(001) Å	S_{BET}, m^2/g	[3]$Vp_{0.98}$ cm^3/g	[4]Vμp mm^3/g	[5]S_{ext} m^2/g
Na-Mont			9.6	87	0.093	12	56
Al2.0		3.1	18.8	219	0.189	67	58
Al1.8		3.01	17.7	206	0.178	44	54
Al1.6		2.30	16.3	171	0.160	54	53
Zr2SR	3.20	4.69	16.2	126	0.144	32	50
Zr5SR	2.75	6.96	16.8	183	0.186	48	71
Zr20SR	2.10	9.63	—	257	0.193	73	108
Zr2R	2.80	6.50	15.5	196	0.176	52	71
Zr5R	2.30	6.95	15.9	264	0.192	79	78
Zr20R	1.96	9.58	—	278	0.203	71	115

[1] See text for sample label information.
[2] After synthesis of Zr oligocations.
[3] $Vp_{0.98}$, Pore volume measured at 0.98 relative pressure (p/p_0).
[4] Micropore volume calculated from t-method.
[5] External surface area calculated from t-method.

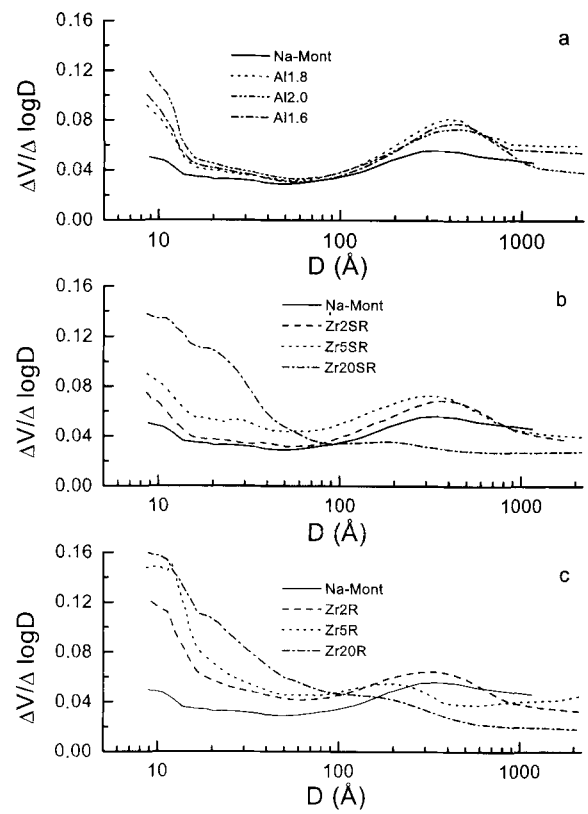

Figure 3. Pore-size distribution: a) Al-series; b) ZrSR-series; c) ZrR-series, where V is volume and D is diameter.

https://doi.org/10.1346/CCMN.2000.0480505 Published online by Cambridge University Press

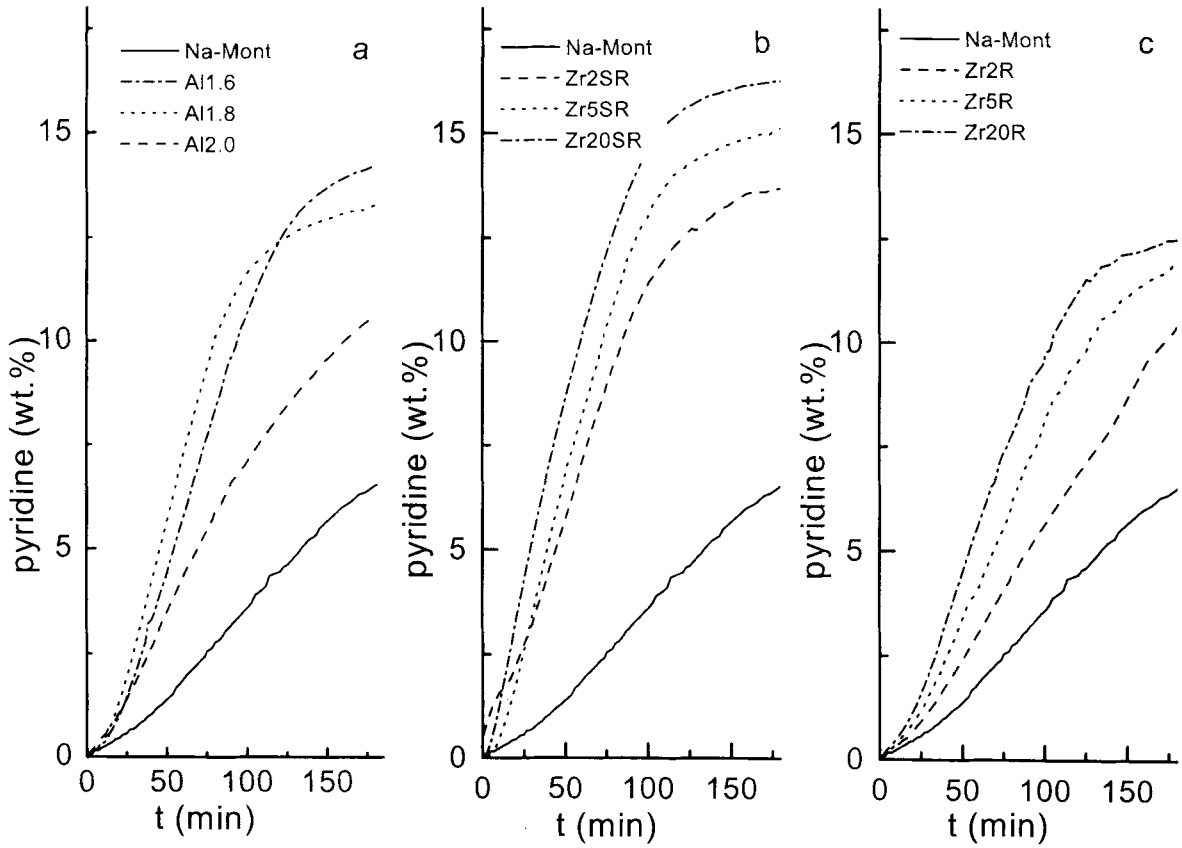

Figure 4. Kinetic curves of pyridine adsorption; amount adsorbed (wt. %) *vs.* time (min): a) Al-series; b) ZrSR-series; c) ZrR-series.

tures, as determined from pyridine thermodesorption experiments.

Most of the pyridine desorbs at 613 K (Table 3), however, an important amount still remains in samples Al1.8, Al1.6, and Zr5SR. These results may be of interest for possible catalytic applications. Curves of dW/dT *vs.* temperature (where W is % weight loss) were obtained (Figure 5), and show that (a) regardless of the metallic oligocation involved, the number of weak acid centers on the pillared clays below 425 K does not deviate significantly from the parent clay. In contrast, strong acidity increases with pillaring. (b) Na-Mont has a significant number of weak acid centers at ~410 K. Thereafter, there is continuous desorption with the temperature, which is related to sites of continuously increasing acid strength. (c) Al-pillared

Table 2. Adsorption-desorption of pyridine.

[1]Material	Total uptake wt. %	Total uptake Sites/g ($\times 10^{-20}$)	Acid-sites density Sites/g ($\times 10^{-20}$)
Na-Mont	8.18	6.22	6.22
Al2.0	11.51	8.77	8.04
Al1.8	13.31	10.15	8.96
Al1.6	14.42	10.99	9.78
Zr2SR	13.72	10.46	9.12
Zr5SR	15.17	11.57	9.46
Zr20SR	16.26	12.40	8.14
Zr2R	11.13	8.48	7.60
Zr5R	12.46	9.50	8.12
Zr20R	12.59	9.60	7.68

[1] See text for sample label information.

Table 3. Acid strength distribution showing the number of sites/g ($\times 10^{-20}$).

[1]Sample	Total	Temperature K 373	423	473	523	573	613
Na-Mont	6.22	4.30	2.10	0.95	0.48	0.24	0.1
Al2.0	8.04	6.88	4.87	2.88	1.52	0.66	0.18
Al1.8	8.96	7.75	5.67	3.67	2.34	1.46	0.90
Al1.6	9.78	8.44	5.11	3.81	2.28	1.28	0.70
Zr2SR	9.12	7.96	5.90	3.74	2.14	1.04	0.28
Zr5SR	9.46	8.43	6.33	4.29	2.68	1.67	0.97
Zr20SR	8.14	7.01	4.37	2.18	1.03	0.21	0.00
Zr2R	7.60	6.66	4.76	2.71	1.35	0.46	0.00
Zr5R	8.12	6.85	4.35	2.29	1.19	0.47	0.05
Zr20R	7.68	6.10	3.31	1.50	0.40	0.00	0.00

[1] See text for sample label information.

https://doi.org/10.1346/CCMN.2000.0480505 Published online by Cambridge University Press

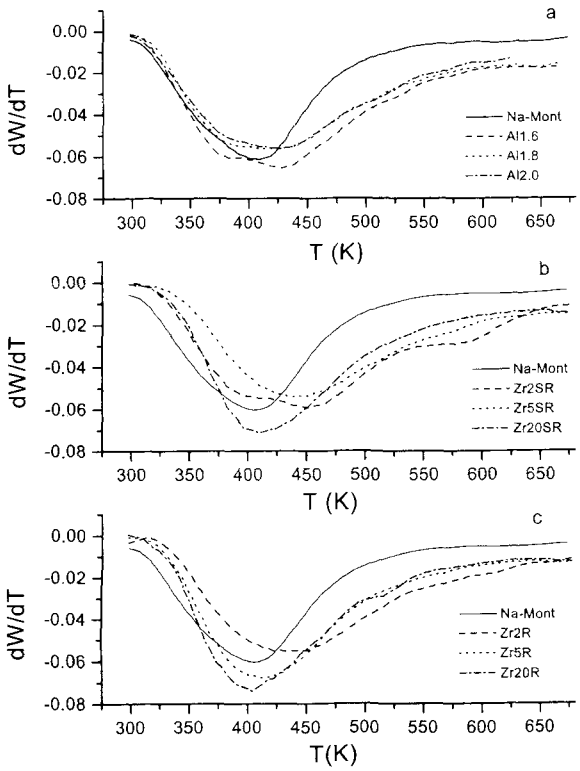

Figure 5. Acid strength distribution, dW/dT *vs.* temperature, in pillared clays: a) Al-series; b) ZrSR-series; c) ZrR-series, where W = weight and T = temperature.

clays have two maxima, the first maximum at a slightly lower temperature than in the parent clay and the second maximum occurring at ~433 K. The intensity of both maxima decreases with the basicity of the hydroxycation-synthesis solution, but they occur at similar temperature, indicating a similar acid strength in the three samples. (d) Zr-pillared clays with metal (Me) cations per g of clay <20 in both series have two peaks at 400 and 450 K, respectively, but, in contrast to the Al-pillared clays (above), the higher-temperature peak gradually disappears, approaching that of the parent material as the Zr content increases.

DISCUSSION

In basic solutions originating from the hydrolysis of aluminum chlorhydrate and in the range of basicity studied here, the polymeric cation most frequently formed is the Keggin (Al_{13}) complex, although, an important contribution from other Al polymers (Schönherr *et al.,* 1983; Jones, 1988) can be expected. An exchange capacity of 61.6 meq/100 g clay, such as that of the parent clay, requires 3.09 wt. % of aluminum for the exchange of the Keggin complex, which occurs in Al2.0 and Al1.8 samples. However, in Al1.6 the amount of metal incorporated by pillaring is only 2.6 wt. % (Table 2) which means that either the incorporated polymeric cations are species with a smaller n/q relation (number of atoms per charge) than the Al_{13} complex or that the exchange was not completed or both. On the other hand, the CEC decreases with the basicity of the pillaring solution (Gutierrez Rios, 1949) and consequently, the number of oligocations incorporated into the parent clay following exchange will vary.

For Zr-pillared clays, the theoretical amount of metal as the tetramer, *i.e.,* $[(Zr(OH)_2{\cdot}4H_2O)_4]^{8+}$, necessary to compensate for the charge of the clay is 2.65 wt. %, and this is far exceeded by the incorporated Zr. When dissolved in water, zyrconil solutions hydrolyze, thereby acidifying the solution. The degree of hydrolysis and further polymerization is related to the concentration and aging conditions (*e.g.,* time and temperature) of the starting solution (Sterte, 1988; Miehé-Brendlé *et al.,* 1997; Bartley, 1988). In our case, the noted differences in the pH of the pillaring solution (Table 1) mean that different Zr species with different n/q values have formed and, hence, different amounts of the species have been incorporated into the clay. Assuming that the exchange was completed for each case, values for n/q were calculated from 0.83 (in SR2) to 1.7 (in SR20 and R20).

Powder X-ray diffractograms of the Al-pillared clays (Figure 1) show slightly different basal spacings, suggesting a difference in the size of the corresponding Al-pillaring cation and indicating the presence of cations such as $[Al_6(OH)_{12}(H_2O)_{12}]$, which is smaller than the Keggin complex. A similar sequence occurs for Zr-pillared clays, except for Zr20SR and Zr20R in which the reflection corresponding to the 001 plane is very weak. Thus, the long range face-to-face association, which is characteristic of the clays, is no longer present and the clay has delaminated during the pillaring process as a consequence of the low pH values involved. Because microporosity remains, (see below), it must be related to short-range aggregates which appear X-ray amorphous.

The N_2 adsorption-desorption isotherms show that all pillared materials have experienced a net increase in porosity, mainly in microporosity, with respect to the parent clay. The difference between the adsorbed amounts by Na-Mont and the corresponding Me-pillared clays at the same relative pressure (P/P_0) is expected to approximate the interlamellar sorption. In Figure 6, these differences are depicted. In all the Al-pillared clays and some of the Zr-pillared clays a type-I curve is obtained. Along with the Langmuir equation applied to the data below 0.4 P/P_0, a value for the N_2 monolayer can be found. These values, converted to a liquid volume, are a measure of the volume of micropores generated by the oligomer intercalation. Values for microporosity (V_L in mm^3/g), calculated from the Langmuir equation, are: Al2.0, 54; Al1.8, 29; Al1.6, 39; Zr2SR, 16; Zr5SR, 39; Zr20SR, 71; ZR2R, 43;

https://doi.org/10.1346/CCMN.2000.0480505 Published online by Cambridge University Press

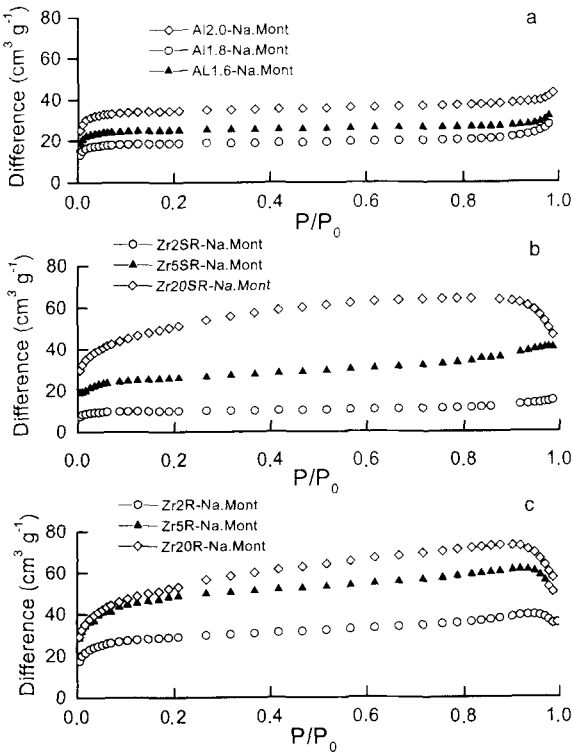

Figure 6. Difference between the amount of N_2 adsorbed at the same pressure by pillared clays and Na-Mont ($cm^3\ g^{-1}$) *vs.* relative pressure (P/P_0): a) Al-series: b) ZrSR-series; c) ZrR-series, at STP.

Zr5R, 71; and Zr20R, 75. These values, added to the microporosity corresponding to Na-Mont (12 mm^3/g) are in good agreement with those calculated from the t-method (Table 1). This may be the result of the adequacy of the method used to study pore-size distributions, and it also shows that the size of the generated pores is <10 Å (the value corresponding to 0.4 P/P_0).

Note that, despite the different cations probably incorporated in the clay, Al-pillared clays and Zr2SR show little change in mesoporosity with respect to the parent material (column 9 in Table 1; Figure 3a). However, in the remaining samples, an additional textural change was produced: the more drastic the synthesis conditions, the greater the changes in meso- and macroporosity as shown in Figure 3b and 3c. As noted above, Zr concentration and aging conditions make the impregnating solution acidic owing to hydrolysis of the tetramer. Thus, the clay stability may be affected, especially for long contact times between the pillaring solution and the clay. A low pH induces a loss of the *d*(001) peak (Table 1) resulting in short-range ordering and produces, besides microporosity, a significant amount of mesoporosity and macroporosity (Figure 3). A type-H4 hysteresis loop corresponding to porosity involved in slit-shaped pores or plate-shaped particles (IUPAC, 1985) persists at low pH, but the extent of the loop is less.

Despite the difference in shape of the kinetic curves of pyridine adsorption, those curves show the S-shaped plot characteristic of an elovichian-type adsorption (Aharoni, 1984) fitting the equation: $dW/dt = a \exp(-bW)$. In the formula, W is the percent weight increase of the sample, t is the time in minutes, *a* and *b* parameters dependent on the sample: *a* is mathematically related to the initial rate of adsorption, and *b* to the process deceleration by a linear increase in the activation energy of adsorption.

For amine adsorption by clays, the low initial sorption rate is associated with a lack of lattice expansion. Attractive forces between the 2:1 layers initially prevent the sorbate from intercalating, but at a threshold pressure (or time), these forces are overcome, the lattice expands, and the 2:1 layers admit gas molecules (Cornet, 1943). The attractive forces between the layers are reduced by this expansion, and thus, further separation requires less energy than for the initial separation, thereby easing the later penetration and increasing the adsorption rate. The threshold pressure was related to a nucleation phenomenon around the periphery of each crystal (Barrer and McLeod, 1954).

In pillaring, a stable porous system develops and there should be no threshold pressure of penetration between the 2:1 layers (Barrer and McLeod, 1955). However, the kinetic curves shown here have the sigmoid form expected for penetration only after nucleation on the expanded phase (Barrer, 1984), and thus a resistance to pyridine diffusion persists.

The number of structural OH groups based in the 2:1 layer calculated on the basis of stoichiometry is estimated at 3.4×10^{21} per g (Ming Yuan *et al.*, 1988). From these OH groups, only a small part can become Brönsted-acid sites during adsorption. In our case, given the structural formula of the clay with a high number of isomorphic substitutions in the octahedral and in the tetrahedral sheets, the number of possible acid sites originating from OH groups must be higher. In addition to these sites, Lewis-acid sites originating from pillars must be added. However, the quantitative measurements of adsorbed pyridine give a number of acid centers about an order of magnitude smaller, suggesting that only some sites are accessible to pyridine. Thus, the product of pillaring may involve both non-expanded montmorillonite and pillared clay. The data are related to differences in the internal diffusion resistance to pyridine and to site heterogeneity, where the activation energy for adsorption varies linearly from one area to another, increasing with coverage (Aharoni, 1984).

No direct relation was found between the content of the micropores and the pyridine adsorption rate. Note that although the mean size of the N_2 molecule is smaller (4.5 Å) than that of pyridine (5.8 Å), the

https://doi.org/10.1346/CCMN.2000.0480505 Published online by Cambridge University Press

shapes of the molecules are different. The pyridine will probably more easily penetrate the pores than N_2. In the clay preconditioning step, the 2:1 layers separate to expose the (001) surface, and allow the oligocation to penetrate. This exposed surface in the raw material is not readily accessible to N_2 when the specific surface area is measured. In contrast, pyridine (or any base) in contact with the clay penetrates between the layers (Barrer, 1989) to occupy all sites, acidic or otherwise, of the original material to give rise to additional surface area. Assuming that this area corresponds to the area made accessible in the preconditioning step, the actual surface area exposed to pillaring must be determined from pyridine rather than by N_2 adsorption. For montmorillonite, the charge density of the interlayer is low (Serratosa *et al.,* 1984), and molecules lie parallel to the silicate layers. Under such conditions, the equivalent cross-sectional area for the adsorbed pyridine molecule is 38.2 Å^2 (McLellan and Harnsberger, 1967). From that value and the quantity adsorbed at equilibrium, a surface area for Na-Mont of 238 m^2/g was calculated. Thus, because the CEC of the original clay is 61.6 meq/100 g, the area per charge unit in the interlayer for pillared crystallites is 64 Å^2. The area required to accommodate every ion, assuming that the intercalated oligocations are either Keggin for Al (d of 9 Å) or tetramer for Zr (d of 5 Å), is 449 and 512 Å^2, respectively. This suggests a distance between pillars of 24 and 26 Å, respectively. With the n/q value of around three times higher than in the tetramer (*e.g.,* 20SR and 20R samples), the distance between pillars should be ~14 Å and no hindrance to N_2 or pyridine penetration is expected, either from this distance relation or from the size of the cations. The resistance to diffusion should arise from the nonexpanded lamellae of the clay fraction remaining in the products.

Once the initial penetration occurs, the number and strength of the acid sites generated through pillaring accounts for the differences among the kinetic curves. Acidity comes from at least two sources: the original clay and the pillaring cation. The clay/pillar bond was also suggested as an acidity source (Ming Yuan *et al.,* 1988), but this is not considered here. For the case where pillaring occurs, the surface occupied by the pillars (for Al_{13} and Zr_4 complexes as pillaring cations) is only 14% of the total surface area. Therefore, an important fraction of the total acidity arises from the clay surface which has been modified by the pillaring process. Low pH values (<4.0) may generate –Si–OH···Me(IV) groups in the tetrahedral sheet of the clay (the lower the pH the more groups are produced), thus enhancing Brönsted acidity (Occelli, 1986). However, delamination of the clay also occurs followed by partial dissolution of the octahedral sheet (Mendioroz *et al.,* 1987; Sun Kou *et al.,* 1998). This results in long range stacking disorder of the sample and in free amorphous-silica products, these imparting their characteristic weak acidity to the resulting material.

Because the pillaring cations differ, other possibilities exist in the generation of acid sites or in the removal of water and protons from the pillars upon calcination, which may affect acidity (Fripiat, 1988). In general, the higher the n/q value, the greater the possibility of generating Lewis-acid sites (the number of unsaturated or low-coordination metal ions being higher) and the smaller the contribution to Brönsted acidity.

Ming Yuan *et al.* (1988) reported that the pillaring process releases Na^+ ions from blocked six-member silicate rings, creating many accessible structural OH groups and possible Brönsted sites, which are accessible to pyridine and which may be eliminated upon heating. If this is the case, the first peak in Figure 5 may be related to the clay substrate and the second to the pillaring cation. As the degree of polymerization of the pillaring cation increases, the number of OH groups from the 2:1 layer involved with pyridinium ions will be smaller, owing to the hindering of silicate rings exposed at the (001) clay surface. The lower temperature peak disappears, whereas the peak from the pillar increases in size provided that the pillaring structure is accessible to pyridine. For Al-pillared clays, a low n/q ratio or an incomplete exchange (*e.g.,* in Al1.6) is related to a high fraction of exposed surface in the clay and, consequently, to a large number of hydroxyl groups (originating from both the 2:1 layer and pillar). Because the oligocation structure $[Al_6(OH)_{12}(H_2O)_{12}]^{6+}$ is open, the possibility of generating Lewis acidity is greater. In contrast, a high n/q value (as in Al2.0), with a larger pillaring cation and more closed structure, results in the opposite effect. Al1.8 occupies an intermediate position.

For Zr-pillared clays, strong acidity increases with n, whereas weak acidity diminishes with q. The acidity of the pillaring solution can affect the structure of the clay surface. Below a certain pH, here 2.75, the octahedral sheet partially dissolves. This produces surface sylanol groups, thus increasing the number of weak acid sites arising from the clay and promoting the loss of pyridine at lower temperatures.

ACKNOWLEDGMENTS

The authors are truly indebted to the CICYT for providing the support for this study under Project Mat95-0143-C02-01. M.R. Sun is grateful to the ICI for granting the scholarship allowing her Ph.D. degree to be completed. We thank Minas de Gador for the kind donation of the smectite sample. Finally we are indebted to M.A. Cheney for his effort in making this work readable.

REFERENCES

Aharoni, C. (1984) Kinetics of adsorption: the S-Shaped z-t plot. *Adsorption Science and Technology,* **1,** 1–29.

Auer, H. and Hofmann, H. (1993) Pillared clays. Characterization of acidity and catalytic properties and comparison with some zeolites. *Applied Catalysis A,* **97,** 23–28.

Barrer, R.M. (1984) Sorption and molecular sieve properties of clays and their importance as catalysts. *Philadelphia Transactions. Royal Society London,* **311,** 333–352.

Barrer, R.M. (1989) Shape selective sorbents based on clay minerals: A review. *Clays and Clay Minerals,* **37,** 385–395.

Barrer, R.M. and McLeod, D.M. (1954) Intercalation and sorption by montmorillonite. *Transactions of the Faraday Society,* **50,** 980–989.

Barrer, R.M. and McLeod, D.M. (1955) Activation of montmorillonite by ion exchange and sorption complexes of tetra-alkylammonium montmorillonites. *Transactions of the Faraday Society,* **51,** 1290–1300.

Barrett, E.P., Joyner, L.G., and Halenda, P.P. (1951) The determination of pore volume and area distribution in porous substances. A computation from N_2 isotherms. *Journal of the American Chemical Society,* **73,** 373–380.

Bartley, G.J. and Burch, R. (1985) Zr-containing pillared interlayer clays. Influence of method of preparation on the thermal and hydrothermal stability. *Applied Catalysis,* **19,** 175–185.

Bartley, J. (1988) Zirconium pillared clays. *Catalysis Today,* **2,** 233–241.

Brunauer, S., Emmett, P.H., and Teller, E. (1938) Adsorption of gases in multimolecular layers. *Journal of the American Chemical Society,* **62,** 1723–1732.

Bodoardo, S., Figueras, F., and Garrone, E. (1994) IR study of Brönsted acidity of Al-pillared montmorillonite. *Journal of Catalysis,* **147,** 223–230.

Bodoardo, S., Chiappetta, R., Onida, B., Figueras, F., and Garrone, E. (1998) Ammonia interaction and reaction with Al-pillared montmorillonite: An IR study. *Microporous and Mesoporous Materials,* **20,** 187–196.

Carrado, K.A., Hayatsu, R., Botto, R.E., and Winans, R.E. (1990) Reactivity of anisoles on clay and pillared clay surfaces. *Clays and Clay Minerals,* **38,** 250–256.

Cornet, I. (1943) Sorption of NH_3 on montmorillonitic clay. *Journal of Chemical Physics,* **11,** 217–226.

Defay, R., Prigogine, I., Bellemans, A., and Everett, D.H. (1966) *Surface Tension and Adsorption.* Longmans, London, 218 pp.

Fripiat, J.J. (1988) High resolution solid state NMR study of pillared clays. *Catalysis Today,* **2,** 281–295.

Gregg, S.J. and Sing, K.S.W. (1982) *Adsorption, Surface Area and Porosity.* Academic Press, London, 244 pp.

Gutierrez Rios, E. (1949) *Bentonitas Españolas.* Consejo Superior de Investigaciones Científicas, Madrid, 32–33.

Hashimoto, K., Hanada, Y., Minami, Y., and Kera, Y. (1996) Conversion of methanol to dimethyl ether and formaldehyde over alumina intercalated in a montmorillonite. *Applied Catalysis A,* **141,** 57–69.

Harkins, W.D. and Jura, G. (1944) Surface of solids. X. Extension of the attractive energy of a solid into an adjacent liquid or film, the decrease of energy with distance, and the thickness of films. *Journal of the American Chemical Society,* **66,** 919–927.

IUPAC, International Pure and Applied Chemistry (1985) Reporting physisorption data for gas/solid systems with special reference to the determination of surface area and porosity. *Pure and Applied Chemistry,* **57,** 609–617.

Jones, S.L. (1988) The preparation and solution chemistry of Al(III) and Zr(IV) pillaring species. *Catalysis Today,* **2,** 209–216.

Lahav, N., Shani, U., and Shabtai, J. (1978) Cross linked smectites I. Synthesis and properties of hydroxy-aluminium montmorillonite. *Clays and Clay Minerals,* **26,** 107–115.

Lippens, B.C. and de Boer, J.W. (1965) Studies on pore systems in catalysis. V. The t method. *Journal of Catalysis,* **4,** 319–323.

McLellan, A.L. and Harnsberger, H.F. (1967) Cross-sectional areas of molecules adsorbed on solids surface. *Journal of Colloid Interface Science,* **23,** 577–599.

Mendioroz, S., Pajares, J.A., Benito, I., Pesquera, C., Gonzalez, F., and Blanco, C. (1987) Texture evolution of montmorillonite under progressive acid treatment: Change from H3 to H2 type of hysteresis. *Langmuir,* **3,** 676–681.

Miehé-Brendlé, J., Khouchaf, L., Baron, J., Le Dred, R., and Tuilier, M.H. (1997) Zr-exchanged and pillared beidellite: Preparation and characterization by chemical analysis, XRD and Zr K EXAFS. *Microporous Materials,* **11,** 171–183.

Ming Yuan, H., Liu, Z., and Enze, M. (1988) Acidic and hydrocarbon catalytic properties of pillared clays. *Catalysis Today,* **2,** 321–338.

Occelli, M.L. (1986) New routes to the preparation of pillared montmorillonite catalysis. *Journal of Molecular Catalysis,* **35,** 377–389.

Occelli, M.L. and Tindwa, R.M. (1983) Physicochemical properties of montmorillonite interlayered with cationic oxyaluminum pillars. *Clays and Clay Minerals,* **31,** 22–28.

Pesquera, C., Gonzalez, F., Benito, I., Mendioroz, S., and Pajares, J.A. (1991) Synthesis and characterization of pillared montmorillonite catalysis. *Applied Catalysis,* **69,** 97–104.

Ross, C.S. and Hendricks, S.B. (1945) *Minerals of the Montmorillonite Group.* U.S. Geological Survey Professional Paper 205-B, Washington, D.C. 23 pp.

Schönherr, S., Gotz, H., Bertram, R., Muller, D., and Gessner, W. (1983) Basic aluminum salt and its solutions. *Zeitschrift für Anorganische und Allgemeine Chemie,* **502,** 113–118.

Serratosa, J.M., Rausell-Colom, J.A., and Sanz, J. (1984) Charge density and its distribution in phillosilicates: Effect of the arrangement and reactivity of the adsorbed species. *Journal of Molecular Catalysis,* **27,** 225–234.

Sterte, J. (1986) Synthesis and properties of titanium oxide cross-linked montmorillonite. *Clays and Clay Minerals,* **34,** 658–664.

Sterte J. (1988) Hydrothermal treatment of hydroxycation precursor solutions. *Catalysis Today,* **2,** 219–230.

Sun Kou, M.R., Mendioroz, S., and Guijarro, I. (1998) A thermal study of Zr-pillared montmorillonite. *Thermochimica Acta,* **323,** 145–157.

Tichit, D., Mountassir, Z., Figueras, F., and Auroux, A. (1991) Control of the acidity of montmorillonites pillared by Al-hydroxy cationic species. In *Preparation of Catalysts V,* G. Poncelet, P.A. Jacobs, P. Grange, and B. Delmon, eds., Elsevier Science Publishers, Amsterdam, 345–353.

Tokarz, M. and Shabtai, J. (1985) Cross-linked smectites. IV. Preparation and properties of hydroxyaluminum-pillared Ce- and La-montmorillonites and fluorinated NH_4^+-montmorillonites. *Clays and Clay Minerals,* **33,** 89–98.

Vaugham, D.E.W., Lussier, R.J., and Magee, J.S. (1981) Stabilized pillared clays. U.S. Patent 4248739.

Yamanaka, S. and Brindley, G.W. (1978) Hydroxy-nickel interlayering in montmorillonite by titration method. *Clays and Clay Minerals,* **26,** 21–28.

Yamanaka, S. and Brindley, G.W. (1979) High surface area solids obtained by reaction of montmorillonite with zyrconyl chloride. *Clays and Clay Minerals,* **27,** 119–124.

E-mail of corresponding author: smendioroz@icp.csic.es

(Received 11 February 1999; accepted 16 April 2000; Ms. 313: A.E. Ljerka Ukrainczyk)